INTERNATIONAL JOURNAL OF HYDROGEN ENERGY 39 (2014) 8374–8384

Available online at www.sciencedirect.com

ScienceDirect

journal homepage: www.elsevier.com/locate/he

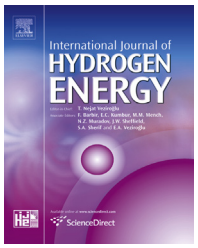

Generalized model of desorption kinetics: Characterization of hydrogen trapping in a homogeneous membrane

*E. Legrand, X. Feaugas, J. Bouhattate**

Laboratoire des Sciences de l'Ingénieur pour l'Environnement, LaSIE UMR CNRS 7356, Bat. Marie Curie, Av. Michel Crépeau, 17042 La Rochelle, France

ARTICLE INFO

Article history:
Received 16 January 2014
Received in revised form
21 March 2014
Accepted 24 March 2014
Available online 19 April 2014

Keywords:
Hydrogen
Permeation
Desorption
Modeling
Trapping
Jump frequencies

ABSTRACT

In this work, we numerically simulated permeations tests on thin martensitic steel membranes using finite elements analyses to determine the behavior of hydrogen during desorption. Starting from a formal model of hydrogen diffusion, we considered cases with one or two kinds of trap sites. We noticed a delay in the desorption of the trapped hydrogen when the trap binding energy rises or when the untrapping jump frequency decreases. The lattice hydrogen may be free from the influence of hydrogen trapping during the desorption if the trapping phenomenon is too weak or too strong. By considering reversible and irreversible trap sites, we notice that the irreversible traps become predominant over the reversible traps. In that case, the lattice hydrogen and reversibly trapped hydrogen behave similarly and may be associated to "diffusible" hydrogen.

Introduction

The phenomenon of hydrogen embrittlement (HE) impacts the durability of materials. Several models have been created to characterize HE, showing that it is initiated by the process of hydrogen diffusion and segregation in materials. To quantify the diffusion of hydrogen at the scale of the membrane, Devanathan and Stachurski [1] designed in 1962 the Electrochemical Permeation (EP) technique. Based on Fick's laws, the electrochemical permeation gives access to diffusivity of hydrogen [1–3], its subsurface concentration, etc. However, the extracted data are representative of an effective behavior due to the lattice behavior and the phenomenon of hydrogen trapping. Since 1949, Darken and Smith [4] determined that Fick's laws did not apply for the diffusion of hydrogen, due to a divergence that was referred as hydrogen trapping. Numerous diffusion models have later been established to consider the phenomenon of hydrogen trapping. Starting with McNabb and Foster [5], the 2nd Fick's law was altered by distinguishing the hydrogen concentrations in lattice sites and trapping sites, respectively noted C_L and C_T. The second Fick's law then became:

* *Corresponding author.*
E-mail address: jamaa.bouhattate@univ-lr.fr (J. Bouhattate).
http://dx.doi.org/10.1016/j.ijhydene.2014.03.191

Nomenclature

D_L	Lattice diffusion coefficient
D_{app}	apparent diffusion coefficient
k_B	Boltzmann constant
T	temperature
C_i	hydrogen concentration in sites i (L = lattice, T = trapped, T_r = reversibly trapped, T_{ir} = irreversibly trapped)
Γ_i	jump rate of an atom in a site i
ν_i	jump frequency of an atom in a site i
N_i	density of sites i
P_i	probability of free neighboring site i
θ_i	occupancy of site i
E_i	binding energy of site i
$<C_i>$	average hydrogen concentration in sites i
C_D	diffusible hydrogen concentration = $C_L + C_{Tr}$

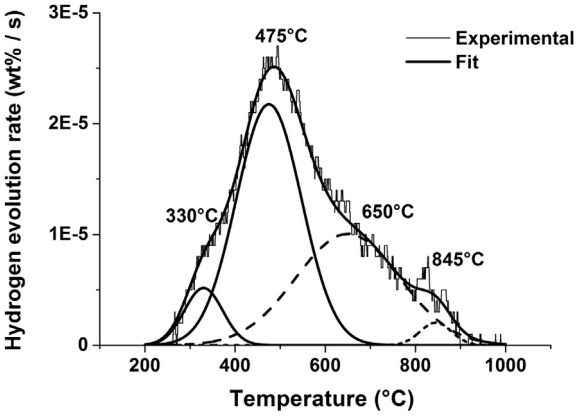

Fig. 1 – Hydrogen desorption profile as a function of the heating rate for quenched and tempered martensite [29].

$$\frac{\partial C_L}{\partial t} + \frac{\partial C_T}{\partial t} = D_L \nabla^2 C_L \quad (1)$$

At this point, the diffusion was controlled by the lattice diffusion coefficient D_L. The trapped hydrogen concentration C_T was expressed as a function of the trapping sites occupancy θ_T and the trapping sites density N_T by Equation (2):

$$C_T = N_T \theta_T \quad (2)$$

Using Equation (2), the trapped hydrogen evolution equation could be calculated using Equation (3), where k and p are reaction constants.

$$\frac{\partial C_T}{\partial t} = N_T k C_L (1 - C_T/N_T) - p C_T \quad (3)$$

In 1970, Oriani [6] considered cases for very low trap occupancies ($\theta_T \ll 1$). From these hypotheses, he replaced the diffusion coefficient D_L in Equation (1) by an apparent diffusion coefficient D_{app} in Equation (4). The diffusion coefficient itself is modified by the equilibrium between the traps and the crystal lattice.

$$\frac{\partial C_L}{\partial t} = D_{app} \nabla^2 C_L \quad \text{with} \quad D_{app} = \frac{D_L}{1 + N_T \frac{k}{p}} \quad (4)$$

The models described by McNabb, Foster and Oriani followed the assumption that the trapped atoms stay in equilibrium with the lattice sites. The hypothesis of hydrogen being trapped in molecular form in voids (instead of atomic form) was developed by several authors [7–9]. The distinction between hydrogen trapped in atomic of molecular form corresponds to the distinction between saturable and non-saturable traps. Whereas saturable traps may only accommodate a finite number of atoms, for example dislocations or vacancies, non-saturable traps do not present this limit, in the case of microvoids. In 1970, Johnson et al. [10] presented a diffusion model by distinguishing the two kinds of traps. More recently, Krom [11] developed the model of McNabb and Oriani to reformulate the diffusion equations. Under the assumptions that the lattice sites occupancy is very low ($\theta_L \ll 1$) and that the trap density is negligible in front of the lattice density, an explicit description of the trapped hydrogen concentrations was obtained:

$$C_T = \frac{N_T}{1 + \frac{N_L}{K_T C_L}} \quad \text{with} \quad K_T = \exp\left[\frac{-\Delta E_T}{k_B T}\right] \quad (5)$$

with N_L the lattice sites density, ΔE_T the difference between the lattice and the trap binding energies, k_B the Boltzmann constant and T the temperature. Recent models considered the same approach to characterize hydrogen trapping [12–14], but we may also note that such result was also obtained by Kirchheim using a statistical approach [15] based on the framework of Fermi–Dirac statistics.

Since the electrochemical permeation measurements are affected by hydrogen trapping, we studied the effects of hydrogen trapping in our previous works [16–18] by using the framework of Krom as a starting point, yet by considering the apparent diffusion coefficient inside the first derivative, as shown in Equation (6). Doing so, the phenomenological couplings of the concentrations gradients were characterized.

$$\frac{\partial C_L}{\partial t} - \nabla \cdot (D_{app} \nabla C_L) = 0 \quad (6)$$

However, all these models have been developed to take into account one type of trap site. These traps were moreover acting as reversible traps, allowing hydrogen to easily escape. Hydrogen traps may be considered as reversible or irreversible, depending on their energy barrier [19]. Several authors [20–24] modified the initial formulation of McNabb and Foster to consider irreversible traps in the equation. Doing so, three contributions of hydrogen concentrations were taken into account; the lattice hydrogen C_L, the reversibly trapped hydrogen C_{Tr} and the irreversibly trapped hydrogen C_{Tir}.

Using the model based on Equation (6), we were able to correlate our model with experimental results from the literature [18]. However, this model only applied to the charging step of permeation. Experimentally, the desorption step gives access to the lattice hydrogen concentration, but also the reversibly trapped hydrogen C_{Tr} The irreversibly trapped hydrogen C_{Tir} is then also calculated [25,26]. A modeling of hydrogen desorption suggests that the consideration of the

three hydrogen contributions is required. In the literature, several works use the Thermal Desorption Spectroscopy (TDS) to quantify hydrogen concentrations in a material, also giving access to binding energies [27,28]. Further comparison with electrochemical permeation results is then feasible [29–31]. Fig. 1 depicts a hydrogen desorption profile as a function of the temperature, from the work of Frappart et al. [29]. The desorption profile may be simulated using only four Gaussian distributions; the two first distributions (solid) correspond to lattice hydrogen desorption, the third (dashed) represents reversibly trapped hydrogen and the last (dotted) corresponds to irreversibly trapped hydrogen, since high temperatures are required to free hydrogen.

Even though the desorption profile may be simulated using only four gaussians, numerous traps with various trap binding energies free hydrogen during desorption. Thus, it is wise to establish the most general model considering n kinds of trap sites. Doing so, the model may be later simplified to take into account a finite number of categories. In that case, the explicit description of the hydrogen concentrations should be avoided to ensure a distinct behavior of the trapped hydrogen concentration contributions.

Diffusion in a model with n traps

The consideration of hydrogen trapping was accomplished in early works by taking into account separate contributions, distinguishing the lattice and trapped hydrogen concentrations. Doing so, Equation (1) was formulated. According to Pressouyre [19], an equilibrium between the lattice and the trapped hydrogen concentrations exists. In that case, the evolution of the trapped hydrogen concentration C_T as a function of time is defined as a function of the temporal derivative of the hydrogen concentrations moving from lattice sites to trap sites, and vice versa. However, considering n types of trap sites, the evolution of C_T is described as the sum of the evolutions of all concentrations in sites with the distinct energy barriers, excluding lattice sites (L). In the following equations, the subscripts i, j, k represent all possible sites, allowing us to give a general model. We write:

$$\frac{\partial C_T}{\partial t} = \sum_{i \neq L} \frac{\partial C_i}{\partial t} \tag{7}$$

where C_i is the hydrogen concentration in a i site of energy E_i. The evolution of the concentration C_i as a function of time depends on all sites that act as a source or sink of hydrogen. This means that we may divide the evolution in two contributions, in Equation (8).

$$\left.\frac{\partial C_i}{\partial t}\right|_{i \neq L} = \sum_j \left.\frac{\partial C_i}{\partial t}\right|_{i \neq L, j \to i} - \sum_j \left.\frac{\partial C_i}{\partial t}\right|_{i \neq L, i \to j} \tag{8}$$

The number of atoms moving from one site to another is proportional to the hydrogen concentration in the source site C_i, the jump rate of a hydrogen atom in the site i: Γ_i, and the probability of getting a free neighbor sink site j: P_j. Obviously, lattice sites also act as sources or sinks and need to be considered as well as sites. The jump rate from a site i to a site j is expressed using a jump frequency ν_i in relation with the vibrational states of hydrogen atoms in the site. The energy barrier E_i also intervenes. Thus, we get Equation (9):

$$\Gamma_i = \nu_i \exp\left[\frac{-E_i}{k_B T}\right] \tag{9}$$

The probability of having a free neighbor site j is calculated from the number on non-occupied sites j divided by the total occupancy of all sites k in the material, thus giving Equation (10):

$$P_j = \frac{N_j(1-\theta_j)}{\sum_k N_k(1-\theta_k)} \tag{10}$$

with N_k the density of sites k and θ_k the occupancy of the k sites, equal to the ratio between the concentration of hydrogen in k sites and their density. Thus, we write the evolution of the hydrogen concentration in an i site with Equation (11):

$$\frac{\partial C_i}{\partial t} = \sum_j \Gamma_j P_i C_j - \sum_j \Gamma_i P_j C_i \tag{11}$$

Finally, by combining Equations (7), (8) and (11), we get the evolution of the total trapped hydrogen concentration for n sites:

$$\frac{\partial C_T}{\partial t} = \sum_{i \neq L} \sum_j \left[\nu_j \exp\left[\frac{-E_j}{k_B T}\right] \frac{N_i(1-\theta_i)}{\sum_k N_k(1-\theta_k)} C_j - \nu_i \exp\left[\frac{-E_i}{k_B T}\right] \frac{N_j(1-\theta_j)}{\sum_k N_k(1-\theta_k)} C_i \right] \tag{12}$$

Equation (12) describes the evolution of the trapped hydrogen concentration for n sites, without any hypothesis on the possibility of hydrogen to escape a site i.

Numerical model

The model with n sites described by Equation (12) is now applied to cases for which we consider a finite number of trap categories. Since numerous parameters appear in the equations describing the evolution of the trapped hydrogen, we first consider the influence of a single type of trap. To perform our investigations, we simulated permeation tests on a metallic membrane, using the model we proposed. The electrochemical permeation setup has already been described in previous works [16,29,30]. In the approach presented here, we focused on the behavior of hydrogen within a membrane containing two types of sites (lattice sites and trap sites with a single energy). Doing so, we implement Equations (1) and (13), the latter being Equation (12) applied to one type of trap site.

$$\frac{\partial C_T}{\partial t} = \nu_L \exp\left[\frac{-E_L}{k_B T}\right] \frac{N_T(1-\theta_T)}{N_L(1-\theta_L)+N_T(1-\theta_T)} C_L - \nu_T \exp\left[\frac{-E_T}{k_B T}\right] \frac{N_L(1-\theta_L)}{N_L(1-\theta_L)+N_T(1-\theta_T)} C_T \tag{13}$$

The simulations are run using the FEA software Comsol Multiphysics, associated with the numerical computing environment MATLAB. We consider the diffusion in a metallic

membrane presented in Fig. 2(a). The dimensions of the membrane are the thickness e_m and the height h_m, with the diffusion occurring along the x-axis. An initial entry side hydrogen concentration C_0 is imposed on the left boundary while a zero concentration C_s is set on the right side boundary. The initial hydrogen concentration inside the membrane is equal to zero, and symmetry conditions are imposed on the boundaries parallel to the diffusion axis.

During electrochemical permeation, the membrane is charged with hydrogen until the hydrogen flux at the exit side attains a steady-state. Then, hydrogen desorption is proceeded by emptying the charging cell. Our numerical analysis follows the same approach; we first apply a strictly positive C_0 concentration to the entry side of the membrane to simulate hydrogen charging. Once the steady-state is reached, C_0 is set to zero to simulate the desorption step. During hydrogen charging, hydrogen may only escape from the right side, while the desorption is possible by both sides.

The lattice diffusion coefficient of hydrogen, the lattice sites density and the lattice binding energy inside the material are respectively noted D_L, N_L and E_L. Since we consider a single type of traps, the trap density and trap binding energy are noted N_T and E_T. Equations (1) and (13) are implemented at each node of the quadratic meshing depicted in Fig. 2(b). During electrochemical permeation tests, the hydrogen flux is measured at the exit side of the membrane. To ensure a sufficient precision, the thickness of the mesh elements decreases towards the exit side of the membrane. The elongation of the mesh elements does not alter the diffusion process, since it is unidirectional.

The parameters of the model are listed in Table 1. Our numerical study considers a martensitic steel membrane 1 mm thick at room temperature, with a lattice diffusion coefficient $D_L = 1.2 \times 10^{-9}$ m^2/s, a lattice sites density $N_L = 2.108 \times 10^5$ mol/m^3 and a trap sites density $N_T = 21$ mol/m^3 [26]. The subsurface concentration C_0 is equal to 1 mol/m^3 during hydrogen charging and it is equal to 0 mol/m^3 for hydrogen desorption. According to Hirth [32], the lattice binding energy is equal to 0.2 eV. Using the classification of Pressouyre [19], hydrogen traps are distinguished between reversible and irreversible traps in terms of their binding energy, with a blurry limit around 0.5 eV. To consider both, we take the trap binding energy between 0.3 and 0.6 eV.

To determine the jump frequency ν, we need to reconsider the energy barrier E_i for an atom to jump. E_i is the Gibbs free energy, and is separated into a contribution of enthalpy H_i and entropy S_i, using Equation (14):

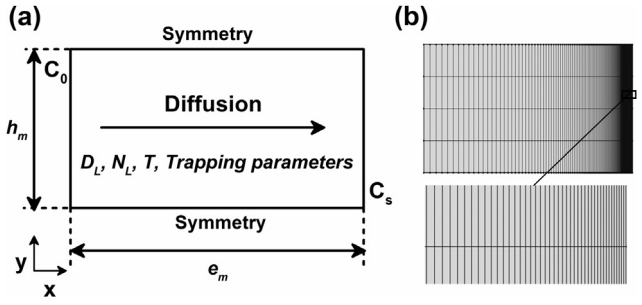

Fig. 2 – (a). Scheme of the model with the boundary conditions and the parameters of the model, (b) quadratic meshing of the membrane.

Table 1 – Parameters of the model.

Parameter	Description	Value(s)
e_m	Thickness of the membrane	1 mm
C_0	Initial entry side concentration	Charging : 1 mol/m^3 Desorption : 0 mol/m^3
C_s	Exit side concentration	0 mol/m^3
D_L	Lattice diffusion coefficient	1.2×10^{-9} m^2/s
N_L	Lattice sites density	2.108×10^5 mol/m^3
N_T	Trap sites density	21 mol/m^3
E_L	Lattice site binding energy	0.2 eV
E_T	Trap site binding energy	0.3–0.6 eV
T	Temperature	300 K

$$E_i = H_i - TS_i \tag{14}$$

Combining Equations (14) and (9), the jump rate Γ is written as:

$$\Gamma_i = \nu \exp\left[\frac{-H_i + TS_i}{k_B T}\right] = \nu \exp\left[\frac{S_i}{k_B}\right] \exp\left[\frac{-H_i}{k_B T}\right] \tag{15}$$

Early works by Einstein [33] and von Smoluchowski [34] led to the relation between the diffusion coefficient and the distance of jump of a particle during a given time. Using these works, the jump rate is defined in Equation (16) [35–37]:

$$\Gamma = \left[\prod_{j=1}^{3N} f_j \Big/ \prod_{j=1}^{3N-1} f_j\right] \exp\left[\frac{-H_i}{k_B T}\right] \tag{16}$$

with f_j the frequencies of stable states, for example tetrahedral or octahedral sites, and f_j' the frequencies of transition states. By identifying Equations (15) and (16), the jump frequency is calculated with Equation (17):

$$\nu = \left[\prod_{j=1}^{3N} f_j \Big/ \prod_{j=1}^{3N-1} f_j\right] \exp\left[\frac{-S_i}{k_B}\right] \tag{17}$$

The entropy S_i is determined using the difference in energies between the ground and the transition states. If we consider diffusion in nickel from the work of Wimmer et al. [36], the ground frequencies are 24.3 THz and 38.7 THz for octahedral and tetrahedral sites, respectively. The transition state frequency between both sites is 47.1 THz. If we refer to the work of Jiang and Carter [38] on bcc Fe, the vibrational frequencies takes values between 29 THz and 58 THz. Yang et al. [39] used a resulting jump frequency of 0.1 THz in their calculations. Since the data from literature presents some discrepancies [40], it is hard to obtain a proper value for the jump frequency of hydrogen. Thus, we chose to take a value in the same order of magnitude of these data; we took ν_L equal to 10 THz.

However, this value only corresponds to the frequency for hydrogen atoms jumping from lattice sites to lattice sites. While this value applies only when the jump is initiated from a lattice site, the question about the jump frequency of an atom inside a trap site arises. Thus, we decided at first to consider a case of equality of the trapping and untrapping

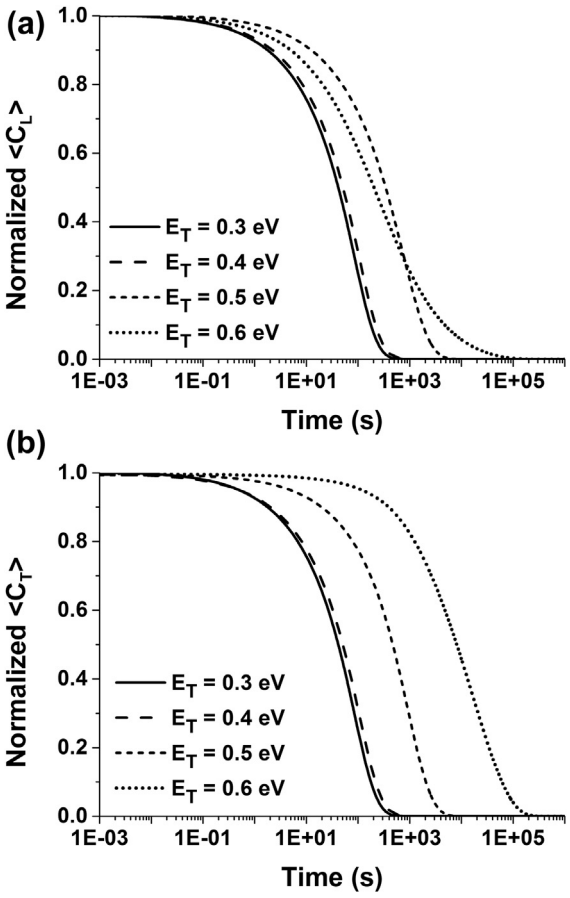

Fig. 3 – Evolution of (a) the normalized average lattice hydrogen desorption, (b) the normalized average trapped hydrogen concentration as a function of time for several trap binding energies during the desorption step.

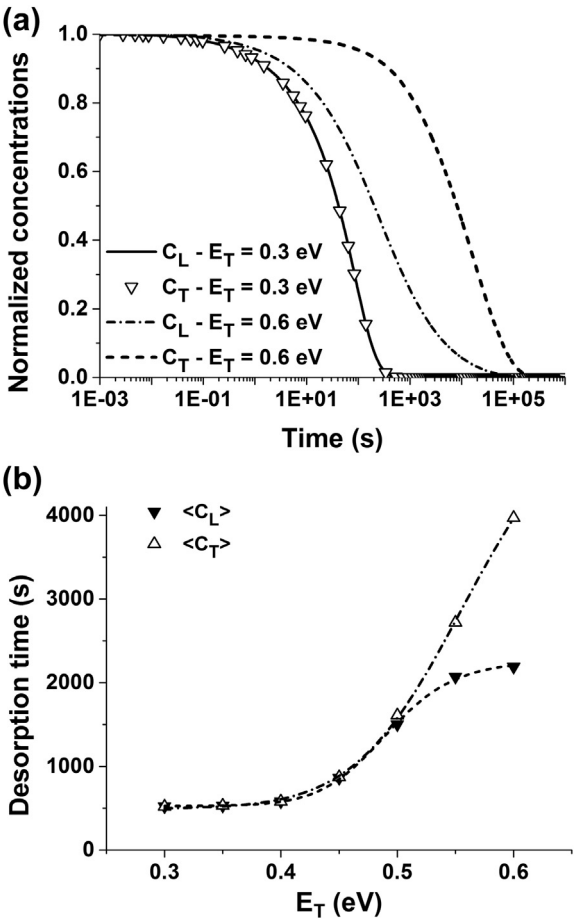

Fig. 4 – (a) Evolution of the normalized average lattice and trapped hydrogen concentrations as a function of time for trap binding energies equal to 0.3 or 0.6 eV. (b). Evolution of the time required to desorb lattice and trapped hydrogen as a function of the trap binding energy.

jump frequencies, to focus on the influence of the trap binding energy E_T. Thus, Equation (13) becomes Equation (18):

$$\frac{1}{\nu_L}\frac{\partial C_T}{\partial t} = \exp\left[\frac{-E_L}{k_B T}\right]\frac{N_T(1-\theta_T)}{N_L(1-\theta_L)+N_T(1-\theta_T)}C_L - \exp\left[\frac{-E_T}{k_B T}\right]\frac{N_L(1-\theta_L)}{N_L(1-\theta_L)+N_T(1-\theta_T)}C_T \quad (18)$$

Results

To characterize the effects of hydrogen trapping on hydrogen desorption, we consider the evolutions of the lattice and trapped hydrogen concentrations. Using our model, we access to the hydrogen concentrations at any point of the membrane. However, for a better comparison, we present the evolutions of the average concentrations, calculated using Equation (19):

$$\langle C_i(t)\rangle = \frac{1}{e_m}\int_0^{e_m} C_i(x,t)dx \quad (19)$$

With the subscript i either replaced by L for the lattice hydrogen concentration, or T for the trapped hydrogen concentration.

Equal jump frequencies for hydrogen trapping and hydrogen untrapping

We ran several calculations to characterize the evolution of the average concentrations during the desorption process. In Fig. 3(a) is depicted the evolution of the normalized average lattice hydrogen concentration $<C_L>$ as a function of time for several trap binding energies. For a low trap binding energy ($E_T = 0.3$ eV), the desorption is completed in 1000 s (~17 min). If E_T is equal to 0.4 eV, the evolution of $<C_L>$ is similar. As soon as the trap binding energy further rises, the desorption is delayed due to hydrogen trapping. In the case of the average trapped hydrogen concentration $<C_T>$ displayed in Fig. 3(b), the trapped hydrogen concentration behaves similarly as the lattice concentration until $E_T = 0.5$ eV. It is only for the highest trap binding energy that a difference between the evolutions of $<C_L>$ and $<C_T>$ emerges. While the trapped hydrogen desorption is further delayed by the trapping, the diminution of the lattice hydrogen concentration begins at earlier times, even before its evolution at $E_T = 0.5$ eV. However, the complete desorption of the lattice hydrogen is also further slowed

down. This evolution means that the trapped hydrogen affects the behavior of the lattice hydrogen. For medium trap binding energies, the lattice hydrogen falls into traps as soon as they are emptied, thus slowing down the lattice desorption process. Yet, when the binding is very strong, the trapped hydrogen escape is slowed down. Consequently, at short times, the lattice hydrogen exits the membrane without being impeded by free traps, and it starts to desorb faster. As soon as the trapped hydrogen starts to escape the membrane, the lattice hydrogen is considerably slowed down by the newly freed traps, thus explaining the final delay in the lattice desorption.

To get a better comparison between the lattice hydrogen concentration and the trapped hydrogen concentration, Fig. 4(a) displays both average concentrations as a function of time for the lowest and the highest trap binding energies. For $E_T = 0.3$ eV, both curves are superimposed; the phenomenon of hydrogen trapping is too weak to influence the lattice diffusion. The behavior of C_T is governed by the lattice diffusion. For $E_T = 0.6$ eV, the desorption of C_T is slower than the desorption of C_L. For a further comparison, Fig. 4(b) depicts the time required to complete the desorption for $<C_L>$ and $<C_T>$ as a function of the trap binding energy E_T. The desorption time corresponds to the time required for the concentration to fall below 1% of its steady-state value. For E_T between 0.3 and 0.4 eV for both concentrations, the desorption time is the same. However, for higher trap binding energies, the desorption of $<C_T>$ is longer. While the lattice hydrogen concentration desorption time seems to stabilize for $E_T \geq 0.55$ eV, the trapped hydrogen concentration desorption time continues its increase.

Depending on the trap binding energy, either the lattice or the trapped hydrogen dictates the global behavior of the desorption. However, we notice that even for a very strong trap binding energy, the desorption duration is very short. According to Pressouyre [19], traps may be considered as irreversible if their binding energy exceeds 0.5 eV. The term of irreversibility supposes that hydrogen cannot escape such trap. In our case, we notice that even for $E_T = 0.6$ eV, we obtain a complete desorption of the trapped hydrogen in less than 3 h. Nonetheless, we made the hypothesis of equal trapping and untrapping frequencies. Such assumption may be wrong, so we also need to characterize the effects of a variation of the untrapping frequency during the desorption.

Distinct jump frequencies for hydrogen trapping and hydrogen untrapping

To consider the influence of the jump frequencies, we have to start from Equation (13) which distinguishes the jump frequency of an atom located in a lattice site from the jump frequency of a trapped atom, respectively noted ν_L and ν_T. We then normalize the equation with the lattice jump frequency ν_L, to obtain Equation (20):

$$\frac{1}{\nu_L}\frac{\partial C_T}{\partial t} = \exp\left[\frac{-E_L}{k_B T}\right]\frac{N_T(1-\theta_T)}{N_L(1-\theta_L)+N_T(1-\theta_T)}C_L - \frac{\nu_T}{\nu_L}\exp\left[\frac{-E_T}{k_B T}\right]\frac{N_L(1-\theta_L)}{N_L(1-\theta_L)+N_T(1-\theta_T)}C_{T'} \quad (20)$$

We maintain the value of the jump frequency in a lattice site; $\nu_L = 10$ THz. To study the effects of the jump frequency in trap sites, we specifically focus on the ratio between ν_T and ν_L. Since the complete clearing out of the membrane is too fast, we may assume that the traps should be harder to escape from. Following this hypothesis, the trapped hydrogen jump frequency should be lower than the lattice hydrogen jump frequency. We ran several calculations by considering the ratio ν_T/ν_L between 10^{-7} and 1. Fig. 5(a) depicts the evolution of the steady-state average lattice hydrogen concentration $<C_L>$ as a function of the ratio between the lattice and the trap jump frequencies, for three trap binding energies E_T. For any E_T, the lattice hydrogen concentration is not affected by a change in the untrapping frequency, and stays equal to $C_0/2$. This is not surprising, since the steady-state solution of Equation (1) is free from the effects of trapping. Concerning the steady-state average concentration, $<C_T>$ is displayed in Fig. 5(b) as a function of ν_T/ν_L for three trap binding energies. In the case of a high trap binding energy, the average trapped hydrogen concentration is equal to the trap density N_T for any ν_T/ν_L below 0.1. A small diminution of the untrapping frequency is enough to completely fill the trap sites. In the case of $E_T = -0.3$ eV, $<C_T>$ only reaches N_T for a low ν_T, while it tends toward zero for higher trap jump frequencies. For the intermediate case ($E_T = 0.45$ eV), $<C_T>$ is equal to N_T below $\nu_T/$

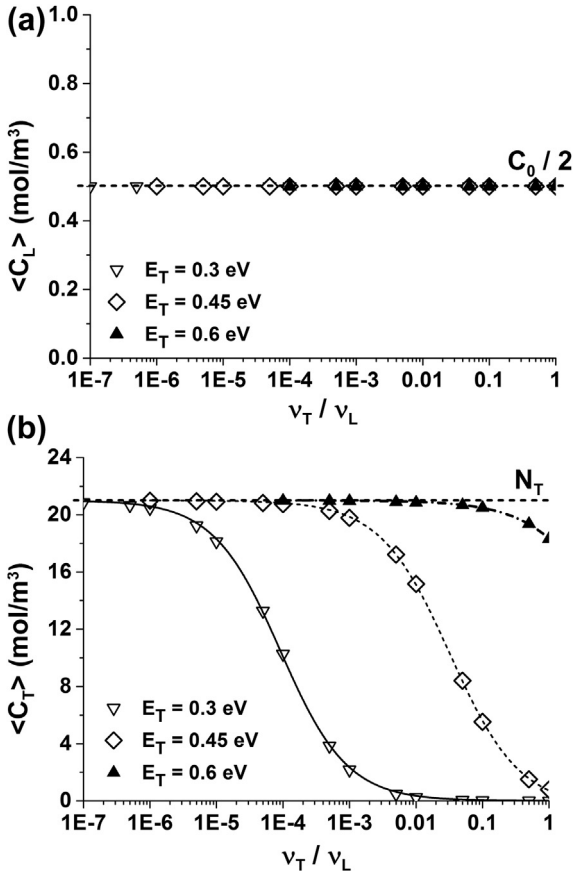

Fig. 5 – Evolution of (a) the average lattice and (b) the trapped hydrogen concentrations at the steady-state after hydrogen charging, as a function of the ratio between the jump frequencies. Trap binding energies $E_T = 0.3$, 0.45 and 0.6 eV.

$\nu_L = 10^{-3}$. When the trap binding energy E_T diminishes, the total fill-up of the trap sites only happens for lower untrapping frequencies. These results show that the untrapping frequency indeed affects the binding of the trapped atoms. When the untrapping frequency is low, hydrogen is strongly bound even for weak trap binding energies.

Since the trapped hydrogen concentration is modified by the untrapping jump frequency ν_T, the behavior of the lattice hydrogen concentration should be questioned. Indeed, the steady-state average lattice hydrogen concentration does not evolve, but the untrapping jump frequency may affect the behavior of $<C_L>$ during the desorption. To answer this question, Fig. 6(a) pictures the evolution of the normalized lattice hydrogen concentration as a function of time during hydrogen desorption, with a medium trap binding energy $E_T = 0.45$ eV, for several untrapping frequencies. The evolution of $<C_L>$ may not be easily explained; while the desorption takes more time when the ratio ν_T/ν_L is equal to 0.01, further diminutions of this ratio reduce the time required for the desorption. Meanwhile, the evolution of the normalized trapped hydrogen concentration is depicted on Fig. 6(b). Unlike $<C_L>$, the trapped hydrogen concentration requires more time to be depleted when ν_T decreases. For example, in the case of the ratio ν_T/ν_L equal to 10^{-6}, $<C_L>$ clears out in about 3 h, while it takes more than 30 years for $<C_T>$. A complete desorption requiring years may be related to irreversible hydrogen trapping. Compared to the time required for the lattice hydrogen to quit the membrane, we may consider the trapped hydrogen as irreversibly bound.

While the behavior of $<C_T>$ follows the evolution of the ratio ν_T/ν_L, we also need to understand the evolution of the average lattice hydrogen concentration $<C_L>$. To do so, Fig. 7 depicts the evolution of the time required for $<C_L>$ to reach 1% of its steady-state value, for three trap binding energies, as a function of the ratio between the jump frequencies. The three curves follow the same trend with a peak shift; for $E_T = 0.3$ eV, the maximum desorption time is reached for $\nu_T/\nu_L = 10^{-6}$. In the case of $E_T = 0.45$ eV, the maximum is at $\nu_T/\nu_L = 10^{-3}$. For a strong trap binding energy, the maximum value is reached at $\nu_T/\nu_L = 10^{-1}$. An increase in the trap binding energy shifts the curve towards the higher trap jump frequencies. This phenomenon can be explained by considering the behavior of hydrogen atoms. In the case of low trap binding energies, hydrogen atoms can easily escape trap sites if the untrapping frequency ν_T is high. In that case, hydrogen trapping does not impede the lattice hydrogen diffusion. If however the untrapping frequency diminishes or the trap binding energy rises, hydrogen trapping also affects the lattice diffusion, thus increasing the desorption time. But, for a strong trap binding energy and a low untrapping frequency, hydrogen atoms cannot escape traps, so they do not affect lattice diffusion anymore, since they are strongly bound. Because of this, the lattice hydrogen is quickly desorbed. Meanwhile, the trapped hydrogen can also exit the membrane at a slower pace, as seen on Fig. 5(b), allowing us to suggest that hydrogen is irreversibly trapped.

Nonetheless, a decrease in the untrapping frequency or a rise of the trap binding energy triggers a similar behavior. Indeed, higher E_T is observed by a shift of the desorption times on the frequency logarithmic scale. While both terms appear undistinguishable, a non-justifiable delay in the desorption in terms of trapping energies could then be referred as a consequence of a lower untrapping frequency. Though, atomistic calculations would give more information on the distinction of the effects of E_T and ν_T.

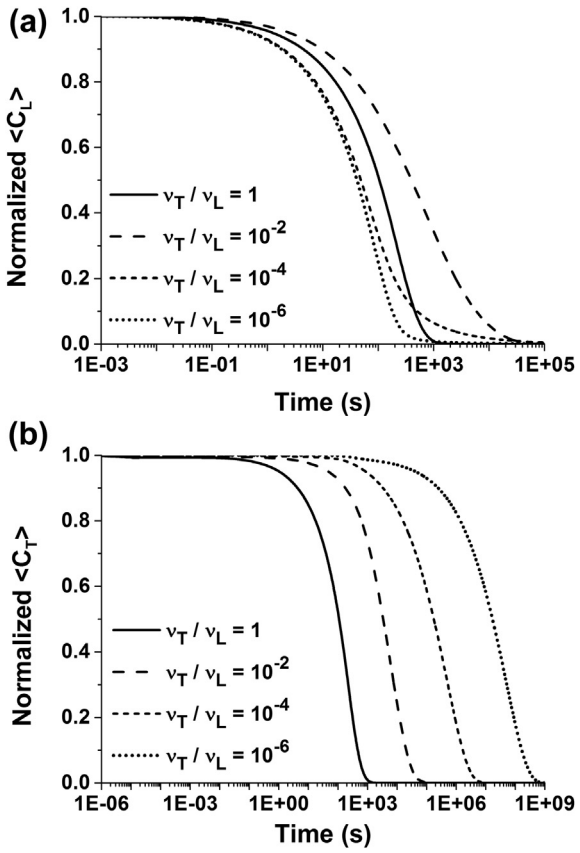

Fig. 6 – Evolution of (a) the normalized average lattice hydrogen concentration, (b) the normalized average trapped hydrogen concentration as a function of time for several jump frequencies from trap sites for a medium trap binding energy $E_T = 0.45$ eV.

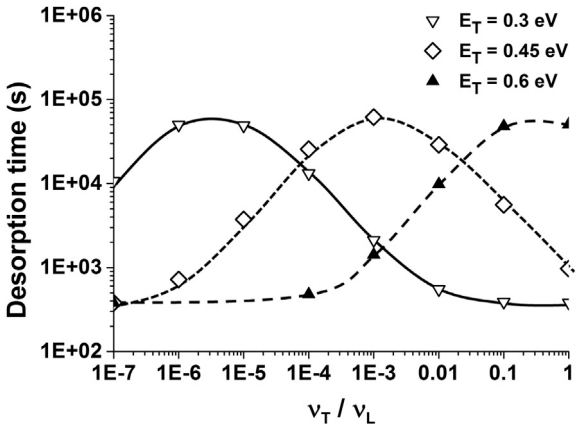

Fig. 7 – Evolution of the desorption time of the lattice hydrogen concentration as a function of the ratio between jump frequencies for three trap binding energies.

Table 2 – Parameters of the model for a three sites approach.

Parameter	Description	Value(s)
e_m	Thickness of the membrane	1 mm
C_0	Initial entry side concentration	Charging : 1 mol/m^3 Desorption : 0 mol/m^3
C_s	Exit side concentration	0 mol/m^3
D_L	Lattice diffusion coefficient	1.2×10^{-9} m^2/s
N_L	Lattice sites density	2.108×10^5 mol/m^3
N_{Tr}	Reversible trap sites density	2000 mol/m^3
N_{Tir}	Irreversible trap sites density	21 mol/m^3
E_L	Lattice site binding energy	0.2 eV
E_{Tr}	Reversible trap site binding energy	0.3 eV
E_{Tir}	Irreversible trap site binding energy	0.6 eV
T	Temperature	300 K
ν_L	Jump frequency of an atom in a lattice site	10 THz
ν_{Tr}	Jump frequency of an atom in a reversible trap site	10 THz
ν_{Tir}	Jump frequency of an atom in an irreversible trap site	10 GHz–10 THz

The characterization of the effects of the untrapping frequency and the trap binding energy are now complete for the approach with two sites. However, as it was illustrated in Fig. 1, three contributions of hydrogen concentrations should be considered. To do so, we now need to distinguish reversible hydrogen trapping from irreversible hydrogen trapping.

Towards a three sites approach

With a three sites approach, we now consider the lattice hydrogen C_L, the reversibly trapped hydrogen C_{Tr} and the irreversibly trapped hydrogen C_{Tir}. Doing so, the total trapped hydrogen concentration is equal to the sum between C_{Tr} and C_{Tir}. Equation (7) becomes Equation (21):

$$\frac{\partial C_T}{\partial t} = \frac{\partial C_{Tr}}{\partial t} + \frac{\partial C_{Tir}}{\partial t} \tag{21}$$

Doing so, the evolution of the variations of C_{Tr} and C_{Tir} are described by taking all sites into account. Thus, Equation (8) is modified and we obtain Equations (22) and (23):

$$\frac{\partial C_{Tr}}{\partial t} = \left.\frac{\partial C_{Tr}}{\partial t}\right|_{L\to Tr} + \left.\frac{\partial C_{Tr}}{\partial t}\right|_{Tir\to Tr} - \left.\frac{\partial C_{Tr}}{\partial t}\right|_{Tr\to L} - \left.\frac{\partial C_{Tr}}{\partial t}\right|_{Tr\to Tir} \tag{22}$$

$$\frac{\partial C_{Tir}}{\partial t} = \left.\frac{\partial C_{Tir}}{\partial t}\right|_{L\to Tir} + \left.\frac{\partial C_{Tir}}{\partial t}\right|_{Tr\to Tir} - \left.\frac{\partial C_{Tir}}{\partial t}\right|_{Tir\to L} - \left.\frac{\partial C_{Tir}}{\partial t}\right|_{Tir\to Tr} \tag{23}$$

If we detail Equations (22) and (23), we get:

$$\frac{\partial C_{Tr}}{\partial t} = \Gamma_L P_{Tr} C_L + \Gamma_{Tir} P_{Tr} C_{Tir} - \Gamma_{Tr} P_L C_{Tr} - \Gamma_{Tr} P_{Tir} C_{Tr} \tag{24}$$

$$\frac{\partial C_{Tir}}{\partial t} = \Gamma_L P_{Tir} C_L + \Gamma_{Tr} P_{Tir} C_{Tr} - \Gamma_{Tir} P_L C_{Tir} - \Gamma_{Tir} P_{Tr} C_{Tir} \tag{25}$$

At this point, we may wonder about possible simplifications of the equations. Indeed, we speak of reversibility and irreversibility of hydrogen trapping. The term "irreversible" suggests that an irreversibly trapped hydrogen atom is unable to escape its trap. Following this assumption, we could remove any contribution involving a jump of an atom located in an irreversible trap. However, the term of irreversibility is to be taken with precaution. Indeed, if we consider the desorption profile from the TDS analysis in Fig. 1, a contribution of the irreversibly trapped hydrogen was clearly defined. This contribution shows that irreversibly trapped hydrogen was able to exit the membrane due to the change of equilibrium. In the context of the TDS, an external supply of heat gave energy to the hydrogen atoms, thus allowing them to escape the

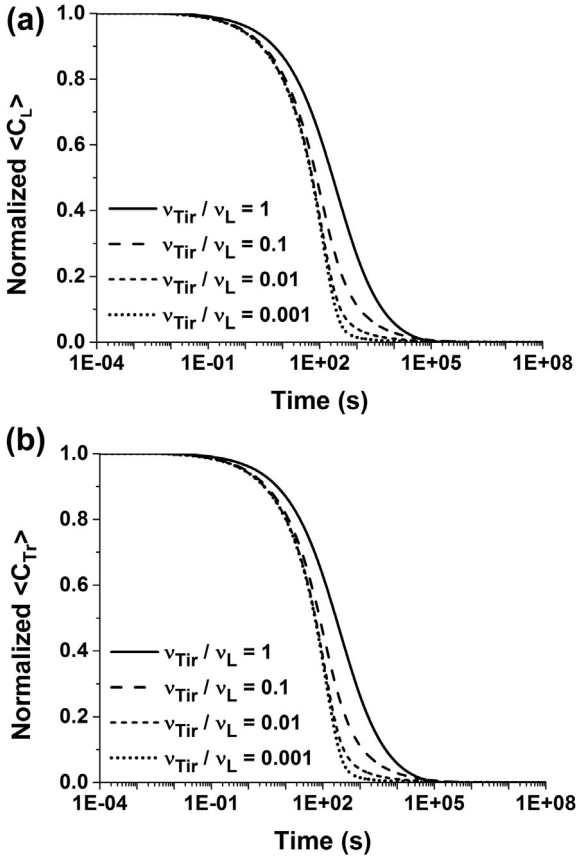

Fig. 8 – Evolution of (a) the normalized lattice hydrogen concentration, (b) the normalized reversibly trapped hydrogen concentration as a function of time for several irreversible trap jump frequencies.

irreversible traps. In our model, such behavior should also be considered. To be sure to take into account any possible change of equilibrium for further calculations, we need to keep the terms relevant to atoms escaping from irreversible traps.

The parameters of the model with three sites are listed in Table 2. We still base our study on a 1 mm-thick martensitic steel membranes at room temperature, with a lattice diffusion coefficient $D_L = 1.2 \times 10^{-9}$ m^2/s and a lattice sites density $N_L = 2.108 \times 10^5$ mol/m^3. The subsurface concentration C_0 is equal to 1 mol/m^3 during hydrogen charging and it is equal to 0 mol/m^3 for hydrogen desorption. Unlike before, we now consider two contributions of trap densities. The trap density calculated by Frappart et al. [26] using the electrochemical permeation corresponds to the irreversible trap density N_{Tir}, so we took N_{Tir} equal to 21 mol/m^3. Concerning the reversible trap density, we chose $N_{Tr} = 2000$ mol/m^3 to remain in a case where $N_L \gg N_{Tr} \gg N_{Tir}$. In terms of energy, we keep the lattice binding energy E_L equal to 0.2 eV. The reversible trap binding energy E_{Tr} is taken equal to 0.3 eV while we use 0.6 eV for the irreversible trap binding energy E_{Tir}. Three jump frequencies now need to be taken into account. First, the jump frequency from a lattice site ν_L is kept at 10 THz. Recent works [41] showed that elastic fields around vacancies do not modify the phonons spectrum, so we may assume that the jump frequency of a reversible trap site is in the same order of magnitude as ν_L. Thus, we also take ν_{Tr} equal to 10 THz. We demonstrated before that a decrease in the jump frequency of a trap site emphasized the effects of trapping. So, we also modify the jump frequency of an irreversible trap site ν_{Tir} to verify its effects.

We ran several calculations to determine the evolutions of the lattice hydrogen concentration and the reversibly trapped hydrogen concentrations as a function of time, for several ν_{Tir} (depicted in Fig. 8). As before, the concentrations are calculated using Equation (19). Fig. 8(a) displays the evolution of the normalized lattice hydrogen concentration as a function of time during the desorption step. When ν_{Tir} diminishes, the time required for $<C_L>$ to be depleted is reduced. If we compare with the evolution of the normalized reversible hydrogen concentration $<C_{Tr}>$ as a function of time, for the same ν_{Tir}, we obtain an identical behavior; the time for $<C_{Tr}>$ to clear out also decreases with the jump frequency.

With the model using only two kinds of sites in Section 4, we demonstrated that for a strong trap binding energy, a low jump frequency suppressed the interactions between the lattice and the trapped hydrogen. Thus, reducing the jump frequency accelerates the desorption of the lattice hydrogen concentration, while slowing down the desorption of the trapped hydrogen. Here, we seem to obtain a similar effect; the lattice hydrogen desorption is sped up by the reduction of ν_{Tir}. Oddly, the reversible trapped hydrogen concentration follows the same behavior, while we could have expected the same evolution as the trapped hydrogen concentration for a low trap binding energy. To question the influence on $<C_{Tir}>$, Fig. 9(a) depicts the evolution of the normalized irreversibly trapped hydrogen concentration as a function of time for several ν_{Tir}. Here, $<C_{Tir}>$ follows the behavior of the trapped hydrogen concentration in Section 4; a reduction of the jump frequency slows down the desorption of $<C_{Tir}>$. To compare the desorption speed, Fig. 9(b) pictures the evolution of the desorption time of $<C_L>$, $<C_{Tr}>$ and $<C_{Tir}>$ as a function of the irreversible trap jump frequency. As observed in Fig. 8, the desorption time for $<C_L>$ and $<C_{Tr}>$ are equal, while $<C_{Tir}>$ is depleted more slowly.

The behavior of $<C_{Tr}>$ follows exactly $<C_L>$. For two kinds of sites, hydrogen trapping was preponderant over the lattice diffusion. Here, we have irreversible trapping dominating lattice diffusion but also reversible trapping. In that way, reversible trapping is not able to influence hydrogen lattice diffusion. When hydrogen is unable to escape irreversible traps due to the jump frequency, $<C_L>$ and $<C_{Tr}>$ behave in the same way, and their desorption is accelerated. Thus, we may consider a "diffusible" hydrogen concentration $<C_D>$ that would be the sum of the lattice and the reversibly trapped hydrogen concentration $<C_L> + <C_{Tr}>$. This behavior had already been considered in the literature; from electrochemical permeation tests, the desorption flux curve is associated with the "diffusible" hydrogen concentration C_D [29,42].

Conclusion

In this work we presented a numerical analysis of the influence of hydrogen trapping during hydrogen desorption. We

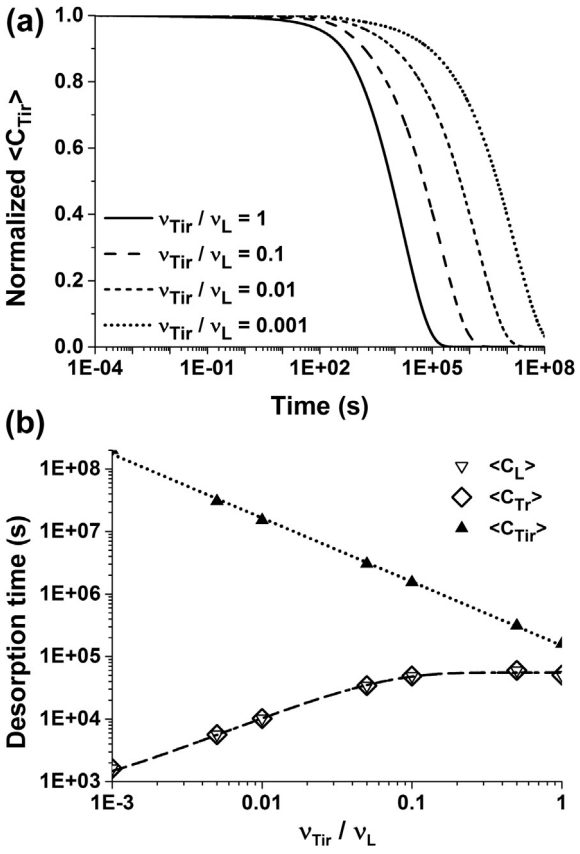

Fig. 9 – (a). Evolution of the normalized irreversibly trapped hydrogen concentration as a function of time for several irreversible trap jump frequencies. (b). Evolution of the desorption time of $<C_L>$, $<C_{Tr}>$ and $<C_{Tir}>$ as a function of ν_{Tir}/ν_L.

simulated electrochemical permeation tests by using a formal model of diffusion we developed for n possible kinds of hydrogen trap sites. That model was then applied to cases with one or two types of trap sites. We extracted the evolutions of the hydrogen concentrations as a function of time to characterize the influence of the parameters of trapping. First, we considered lattice hydrogen and one type of trap site. Considering equal jump frequencies for hydrogen trapping and for hydrogen untrapping, we observed a fast desorption, even for high trap binding energies. We then studied the influence of the untrapping frequency on desorption. A reduction of that frequency led to a considerable slowdown of the trapped hydrogen desorption. Also, we noticed that the lattice hydrogen was detained only when hydrogen trapping was able to affect its diffusion. With too weak or too strong hydrogen trapping, the lattice hydrogen is not affected. We then extended our approach to consider two types of trap sites: reversible traps and irreversible traps. Doing so, we determined that the reversibly trapped hydrogen is dominated by the irreversibly trapped hydrogen. In that way, the lattice and the reversibly trapped hydrogen may be considered as a single concentration, called the "diffusible" concentration.

This study is the first step of characterization for hydrogen desorption. We worked here with a homogeneous membrane and noticed total desorption of all hydrogen concentrations. However, taking into account microstructural heterogeneities should lead to a different behavior of the irreversibly trapped hydrogen.

Acknowledgment

The authors wish to thank the ANR CRISTALHYD 13-JS09-0015 for its financial support, and also Arnaud Metsue and Abdelali Oudriss for their fruitful discussion and comparison with their work.

REFERENCES

[1] Devanathan MAV, Stachurski Z. The adsorption and diffusion of electrolytic hydrogen in palladium. Pc R Soc A 1962;270:90–102.
[2] McBreen J, Nanis L, Beck W. A method for determination of the permeation rate of hydrogen through metal membranes. J Electrochem Soc 1966;113:1218–22.
[3] Boes N, Züchener H. Electrochemical methods for studying diffusion, permeation and solubility of hydrogen in metals. J Less Common Met 1976;49:223–40.
[4] Darken LS, Smith RP. Behavior of hydrogen in steel during and after immersion in acid. Corros 1949;5:1–15.
[5] McNabb A, Foster PK. A new analysis of the diffusion of hydrogen in iron and ferritic steels. Trans Metall AIME 1963;227:618–27.
[6] Oriani RA. The diffusion and trapping of hydrogen in steel. Acta Metall 1970;18:147–57.
[7] Chew B. A void model for hydrogen diffusion in steel. Met Sci 1971;5:195–200.
[8] Allen-Booth DM, Hewitt J. A mathematical model describing the effects of micro voids upon the diffusion of hydrogen in iron and steel. Acta Metall 1974;22:171–5.
[9] Kass WJ. Comments on 'a mathematical model describing the effects of microvoids upon the diffusion of hydrogen in iron and steel'. Scr Metall 1974;8:763–7.
[10] Johnson HH, Quick N, Kumnick AJ. Hydrogen trapping mechanisms by permeation techniques. Scr Metall 1979;13:67–72.
[11] Krom AHM, Bakker AD. Hydrogen trapping models in steel. Metall Mater Trans B 2000;31:1475–82.
[12] Castaño-Rivera P, Ramunni VP, Bruzzoni P. Numerical study of hydrogen trapping: application to an API 5L X60 steel. ISRN Mater Sci 2012;2012. 945235.
[13] Svoboda J, Fischer FD. Modelling for hydrogen diffusion in metals with traps revisited. Acta Mater 2012;60:1211–20.
[14] Fischer FD, Mori G, Svoboda J. Modelling the influence of trapping on hydrogen permeation in metals. Corros Sci 2013;76:382–9.
[15] Kirchheim R. Hydrogen solubility and diffusivity in defective and amorphous metals. Prog Mater Sci 1988;32:261–325.
[16] Bouhattate J, Legrand E, Feaugas X. Computational analysis of geometrical factors affecting experimental data extracted from hydrogen permeation tests: I – consequences of trapping. Int J Hydrogen Energy 2011;36:12644–52.
[17] Legrand E, Bouhattate J, Feaugas X, Garmestani H. Computational analysis of geometrical factors affecting experimental data extracted from hydrogen permeation tests: II – consequences of trapping and an oxide layer. Int J Hydrogen Energy 2012;37:13574–82.
[18] Legrand E, Oudriss A, Frappart S, Creus J, Feaugas X, Bouhattate J. Computational analysis of geometrical factors affecting experimental data extracted from hydrogen permeation tests: III – comparison with experimental results from the literature. Int J Hydrogen Energy 2014;39:1145–55.
[19] Pressouyre GM. A classification of hydrogen traps in steel. Metall Trans A 1979;10:1571–3.
[20] Iino M. A more generalized analysis of hydrogen trapping. Acta Metall 1982;30:367–75.
[21] Lebond JB, Dubois D. A general mathematical description of hydrogen diffusion in steels-I. Derivation of diffusion equations from Boltzmann-type transport equations. Acta Metall 1983;31:1459–69.
[22] Leblond JB, Dubois D. A general mathematical description of hydrogen diffusion in steels-II. Numerical study of permeation and determination of trapping parameters. Acta Metall 1983;31:1471–8.
[23] Turnbull A, Carroll MW, Ferris DH. Analysis of hydrogen diffusion and trapping in 13% chromium martensitic stainless steel. Acta Metall 1989;37:2039–64.
[24] Turnbull A, Carroll MW. The effect of temperature and H_2S concentration on hydrogen diffusion and trapping in a 13% chromium martensitic stainless steel in acidified NaCl. Corros Sci 1990;30:667–79.
[25] Zakroczymski T. Adaptation of the electrochemical permeation technique for studying entry, transport and trapping of hydrogen in metals. Electrochem Acta 2006;51:2261–6.
[26] Frappart S, Feaugas X, Creus J, Thebault F, Delattre L, Marchebois H. Study of the hydrogen diffusion and segregation into Fe–C–Mo martensitic HSLA steel using electrochemical permeation test. J Phys Chem Solids 2010;71:1467–79.
[27] Lee JY, Lee SM. Hydrogen trapping phenomena in metals with B.C.C. and F.C.C. crystals structures by the desorption thermal analysis technique. Surf Coat Tech 1986;28:301–14.
[28] Wang M, Akiyama E, Tsuzaki K. Effect of hydrogen on the fracture behavior of high strength steel during slow strain rate test. Corros Sci 2007;49:4081–97.
[29] Frappart S, Oudriss A, Feaugas X, Creus J, Bouhattate J, Thébault F, et al. Hydrogen trapping in martensitic steel

investigated using electrochemical permeation and thermal desorption spectroscopy. Scr Mater 2011;65:859–62.
[30] Oudriss A, Creus J, Bouhattate J, Conforto E, Berziou C, Savall C, et al. Grain size and grain-boundary effects on diffusion and trapping on hydrogen in pure nickel. Acta Mater 2012;60:6814–28.
[31] Oudriss A, Creus J, Bouhattate J, Savall C, Peraudeau B, Feaugas X. The diffusion and trapping of hydrogen along the grain boundaries in polycrystalline nickel. Scr Mater 2012;66:37–40.
[32] Hirth JP. Effects of hydrogen on the properties of iron and steel. Metall Trans A 1980;11:861–90.
[33] Einstein A. Über die von der molekularkinetischen Theorie des Wärme geforderte Bewegung von in ruhenden Flüssigkeiten suspendierten Teilchen. Ann Phys Berl 1905;322:549–60.
[34] Smoluchowski M. Zur kinetischen Theorie des Brownschen Molekularbewegung und der Suspensionen. Ann Phys Berl 1909;6(326):756–80.
[35] Wert C, Zener C. Interstitial atomic diffusion coefficients. Phys Rev 1949;76:1169–75.
[36] Wimmer E, Wolf W, Sticht J, Saxe P, Geller C, Najafabadi R, et al. Temperature-dependent diffusion coefficients from ab initio computations: hydrogen in nickel. Phys Rev B 2008;77:134305.
[37] Amman M. Diffusion in minerals of the earth's lower mantle: constraining rheology from first principles. Thesis. UCL; 2010. p. 465.
[38] Jiang DE, Carter EA. Diffusion of interstitial hydrogen into and through bcc Fe from first principles. Phys Rev B 2004;70:064102–9.
[39] Yang K, Cao M, Wan X, Shi C. Analysis of hydrogen diffusion in metals with trapping under local equilibrium assumption. Chin J Met Sci Tech 1990;6:162–6.
[40] You YW, Kong XS, Wu XB, Xu YC, Fang QF, Chen JL, et al. Dissolving, trapping and detrapping mechanisms of hydrogen in bcc and fcc transition metals. AIP Adv 2013;3:012118.
[41] Metsue A, Bouhattate J, Osman Hoch B, Legrand E, Feaugas X. Formation et diffusion des lacunes dans le nickel: etude par calculs ab initio. In: Colloque Plasticité; 2013. Paris.
[42] Leblond JB, Nejem D, Dubois D, Talbot-Besnard S. Experimental and numerical study of diffusion and trapping of hydrogen in plastically deformed A508.Cl.3 steel at room temperature. Acta Metall 1987;35:1703–14.